climate

MDPI

Article

The Effects of Historical Housing Policies on Resident Exposure to Intra-Urban Heat: A Study of 108 US Urban Areas

Jeremy S. Hoffman [1,2,*], Vivek Shandas [3] and Nicholas Pendleton [1,2]

1 Science Museum of Virginia, Richmond, VA 23220, USA; pendletonnv@mymail.vcu.edu
2 Center for Environmental Studies, Virginia Commonwealth University, Richmond, VA 23220, USA
3 Nohad A. Toulan School of Urban Studies and Planning, Portland State University, Portland, OR 97201, USA; vshandas@pdx.edu
* Correspondence: jhoffman@smv.org

Received: 5 November 2019; Accepted: 3 January 2020; Published: 13 January 2020

Abstract: The increasing intensity, duration, and frequency of heat waves due to human-caused climate change puts historically underserved populations in a heightened state of precarity, as studies observe that vulnerable communities—especially those within urban areas in the United States—are disproportionately exposed to extreme heat. Lacking, however, are insights into fundamental questions about the role of historical housing policies in cauterizing current exposure to climate inequities like intra-urban heat. Here, we explore the relationship between "redlining", or the historical practice of refusing home loans or insurance to whole neighborhoods based on a racially motivated perception of safety for investment, with present-day summertime intra-urban land surface temperature anomalies. Through a spatial analysis of 108 urban areas in the United States, we ask two questions: (1) how do historically redlined neighborhoods relate to current patterns of intra-urban heat? and (2) do these patterns vary by US Census Bureau region? Our results reveal that 94% of studied areas display consistent city-scale patterns of elevated land surface temperatures in formerly redlined areas relative to their non-redlined neighbors by as much as 7 °C. Regionally, Southeast and Western cities display the greatest differences while Midwest cities display the least. Nationally, land surface temperatures in redlined areas are approximately 2.6 °C warmer than in non-redlined areas. While these trends are partly attributable to the relative preponderance of impervious land cover to tree canopy in these areas, which we also examine, other factors may also be driving these differences. This study reveals that historical housing policies may, in fact, be directly responsible for disproportionate exposure to current heat events.

Keywords: urban heat islands; environmental justice; climate change; redlining

1. Introduction

No other category of hazardous weather event in the United States has caused more fatalities over the last few decades than extreme heat [1]. In fact, extreme heat is the leading cause of summertime morbidity and has specific impacts on those communities with pre-existing health conditions (e.g., chronic obstructive pulmonary disease, asthma, cardiovascular disease, etc.), limited access to resources, and the elderly [2–4]. Excess heat limits the human body's ability to regulate its internal temperature, which can result in increased cases of heat cramps, heat exhaustion, and heatstroke and may exacerbate other nervous system, respiratory, cardiovascular, genitourinary, and diabetes-related conditions [5]. As heat extremes in urban areas become more common, longer in duration, and more intense across the US and globe [6,7] due to unmitigated human emissions of

heat-trapping gases from fossil fuels [8] as well as urban expansion [9], the number of deaths and attendant illnesses are expected to increase around the US [10].

Urban landscapes amplify extreme heat due to the imbalance of low-slung built surfaces to natural, non-human manufactured landscapes [11,12]. This urban heat island effect can cause temperatures to vary as much as 10 °C within a single urban area [13], even without comparison to a "traditional" rural baseline for assessing UHI. Others, including Li et al. (2017), found that the density of total impervious surface area (ISA) is a major predictor for land surface temperatures, or the "surface urban heat island" studied here [14]; yet others describe the apparent cooling effects of urban green spaces. In general, greenspace, trees, or water bodies within a city have been correlated with cooler land surface temperatures (LST), and more greenspace or water is related to lower urban LST at the location of that greenspace [15–18]. Hamstead et al. (2016) studied the role of landscape composition on surface temperatures by dividing New York City into 22 classes at 3-m resolution and identifying the specific ranges of land surface temperature represented within each class [19]. The authors conclude that urban areas contain discernable "classes" of form—the integration of land use and land cover—and that those sets have "distinct temperature signatures".

Emerging research suggests that many of the hottest urban areas also tend to be inhabited by resource-limited residents and communities of color [20,21], underscoring the emerging lens of environmental justice as it relates to urban climate change and adaptation. In one study, Voelkel and others (2018) found that residents living in neighborhoods with higher racial diversity, extreme poverty, and lower levels of formal education were statistically more likely to be exposed to greater heat—the neighborhood heat effect [21]. Still other studies have found that those with the least access to resources, more advanced in age, and people with pre-existing face some of the greatest burden [22]. While the evidence about the distributional implications of heat waves mounts, we still do not have a clear uniting principle to explain consistent patterns between an emerging challenge like intra-urban heat and observable records of excess mortality and morbidity among underserved populations. If heat varies across urban environments, then why are communities of color and resource-limited communities living in the hottest areas? Could a plausible explanation be the presence of past urban planning programs and housing policies that have heightened disproportionate exposure to intra-urban heat in US cities?

The present study further examines the relationship between present-day spatial patterns of inequitable exposure to intra-urban heat and historical housing policies, which were applied to many US cities in the early 20th century. We specifically examine maps generated by the Home Owners' Loan Corporation's (HOLC) practice of "redlining" [23,24] in the 1930s. As part of a national program to lift the US out of a recession, HOLC refinanced mortgages at low interest rates to prevent foreclosures, and in the process created color-coded residential maps of 239 individual US cities with populations over 40,000. HOLC maps distinguished neighborhoods that were considered "best" and "hazardous" for real estate investments (largely based on racial makeup), the latter of which was outlined in red, leading to the term "redlining." These "Residential Security" maps reflect one of four categories ranging from "Best" (A, outlined in green), "Still Desirable" (B, outlined in blue), "Definitely Declining" (C, outlined in yellow), to "Hazardous" (D, outlined in red), relating directly to subsequent access to mortgage lending and at least partially to the racial makeup of that neighborhood.

Though redlining was banned in the US as part of the Fair Housing Act of 1968, a majority of those areas deemed "hazardous" (and subsequently "redlined") remain dominantly low-to-moderate income and communities of color, while those deemed "desirable" remain predominantly white with above-average incomes [24]. Those living in redlined areas experienced reduced credit access and subsequent disinvestment, leading to increased segregation and lower home ownership, value, and personal credit scores, even when compared to those similar-sized US cities that did not receive a HOLC map [23]. Increasingly evident is the legacy of these historic policies in racial disparities in health care, access to healthy food, incarceration, resources allotted for schools, and public infrastructure

investment such as the privileging of the suburban highway system at the expense of the city's public transportation [25].

Similarly, as areas that received severely limited real estate investment over time, we might expect those areas to have fewer environmental amenities that help to clean and cool the air, including urban tree canopy [26]. Recent studies describe the increased likelihood that those who are poor and communities of color are more likely living in areas with fewer trees and poorer air quality [27,28]. At the same time, the extent to which these policies may have resulted in environmental disparity as a consequence of systematic disinvestment nationally largely remains an open question. We seek here to assess if evidence of disproportionate environmental stressors (specifically anomalous urban land surface temperatures) exists through the lens of these long-term housing policies, and if a national-scale signal varies by region in the US.

By assessing HOLC maps from aggregated urban areas in the United States (Figure 1) in relation to the relative anomaly of land surface temperature within and outside redlined areas, we ask two questions: (1) do historical policies of redlining help to explain current patterns of exposure to intra-urban heat in US cities? and (2) how do these patterns vary by geographic location of cities? Our intent is not to explain why precisely these patterns exist; instead, we seek to describe their relation through spatial analysis of historical redlining maps and present-day warm season intra-urban land surface temperature anomalies. By examining these patterns, we aim to assess how current patterns of intra-urban heat inequities may result from a combination of historical policies that may be further exacerbated by present-day planning practices that fail to center communities that have been historically underserved in adaptation and mitigation of these patterns.

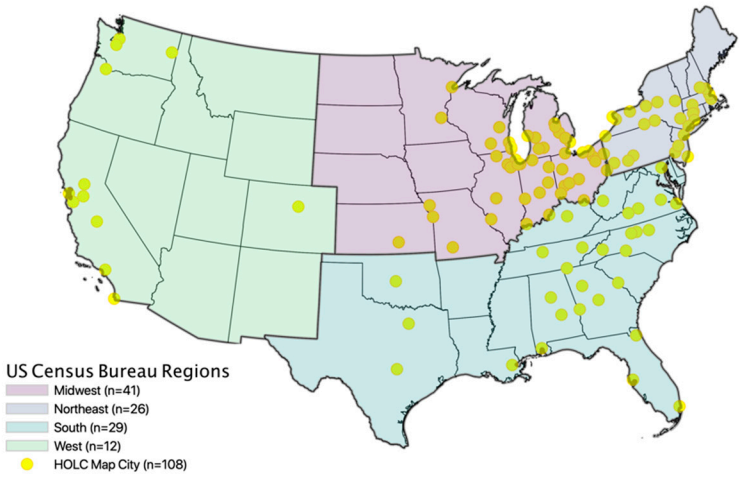

Figure 1. Map of 108 US cities with HOLC Residential Security maps included in this study. These areas may include several smaller-area HOLC maps that have been aggregated into a larger urban area (Supplementary Materials I).

2. Materials and Methods

We use the University of Richmond's Digital Scholarship Lab's "Mapping Inequality" database (Figure 2a, Richmond, VA, USA, [29]) to download each available city's HOLC map shapefile individually (n = 239). To make analysis of Landsat-derived LST maps less computationally complex, we then condense the 239 unique HOLC maps into a database of 108 US cities or urban areas that overlap within Landsat 8 imagery tiles, and excluding any cities that were not mapped with at least one of all four HOLC security rating categories (n = 4). In some cases, HOLC map shapefile boundaries needed to remove overlapping security rating boundaries, boundary crossings over bodies of water, and to merge overlapping maps drawn in the same generalizable urban area and/or because they were drawn during different years (Supplementary Materials I).

We assess patterns of intra-urban land surface temperatures in the 108 HOLC areas using readily-accessible Landsat 8 satellite-derived northern hemisphere summertime (June–August) land surface temperatures (LSTs) following accepted United States Geological Survey calculation protocol (30 × 30 m resolution, TIRS Band 10, Normal Difference Vegetation Index [NDVI] emissivity corrected LST, Figure 2b [20,30,31]. This LST method relies on transforming raw Landsat 8 TIRS Band 10 data into top-of-atmosphere spectral radiance and then into at-sensor brightness temperatures. LST is then calculated by correcting the at-sensor brightness temperatures by surface emissivity calculated from the NDVI (derived from Bands 4 and 5 [30]). LST maps were only generated from imagery that satisfied a threshold for less than 10 percent scene cloud coverage and had to have been collected in the northern hemisphere summertime between 2014 and 2017. While these LST descriptions of intra-urban heat are coarse in spatial resolution and not the most representative of human-level, experiential air temperatures which are better resolved by dense networks of air temperature and humidity monitors [13,32], LST maps such as these have been widely applied to questions of large-scale patterns related to urban land use and heat-related public health outcomes for individual US cities [20,33].

We then use Zonal Statistics in ESRI's ArcGIS Spatial Analyst toolbox to estimate the mean of the derived Landsat 8 LSTs within each individual HOLC security rating polygon within a given urban area (e.g., Figure 2b,c). We then estimate each individual HOLC security rating polygon's land surface temperature anomaly from the area-wide mean LST from all HOLC security rating polygons (referred to as δLST, Equation (1)).

$$\delta\mathrm{LST}_{area,\ polygon} = \overline{\mathrm{LST}_{area,\ polygon}} - \overline{\mathrm{LST}_{area,\ all\ polygons}} \quad (1)$$

This δLST estimate gives us the ability to show relatively how much warmer or cooler a particular HOLC security rating polygon is from the entire set of HOLC security rating polygons for a given urban area, and then compare these anomalies between cities in a quantitative manner.

We also estimate average percent developed impervious surface land cover [34] and tree canopy cover [35] within each HOLC polygon (Figure 2e,g) in each urban area as derived from the National Land Cover Database (NLCD) 2011 [36]. NLCD tree canopy percent is a 30 m raster dataset covering the coterminous United States, providing continuous percent tree canopy estimates derived from multi-spectral Landsat imagery for each 30 m pixel. NLCD imperviousness reports the percentage of urban developed surfaces that is impervious over every 30 m pixel in the coterminous United States and beyond. These estimates of underlying land use and overlying tree canopy may not sum to 100 percent, as tree canopy can exist over all land use types within a HOLC polygon and not all land use is necessarily impervious.

To compare δLST variations within and among HOLC security ratings between cities, we then average the estimated δLST by HOLC security rating category within each city. This binning by HOLC category yields how δLST varies between HOLC security ratings within each city. We then binned the δLSTs for each city at the national scale (n = 108) and by US Census Bureau regions: Northeast (n = 26), South (n = 29), Midwest (n = 41), and Western (n = 12). To estimate the significance of mean temperature differences between the HOLC security ratings by region and nationally, we apply a post-hoc ANOVA multiple comparisons test known as Tukey's Honest Significant Differences (HSD) Test. Tukey's HSD test estimates differences among group sample means for statistical significance. This pairwise post-hoc ANOVA test determines the statistical significance of differences between the mean of all pairs of group means using a studentized range distribution.

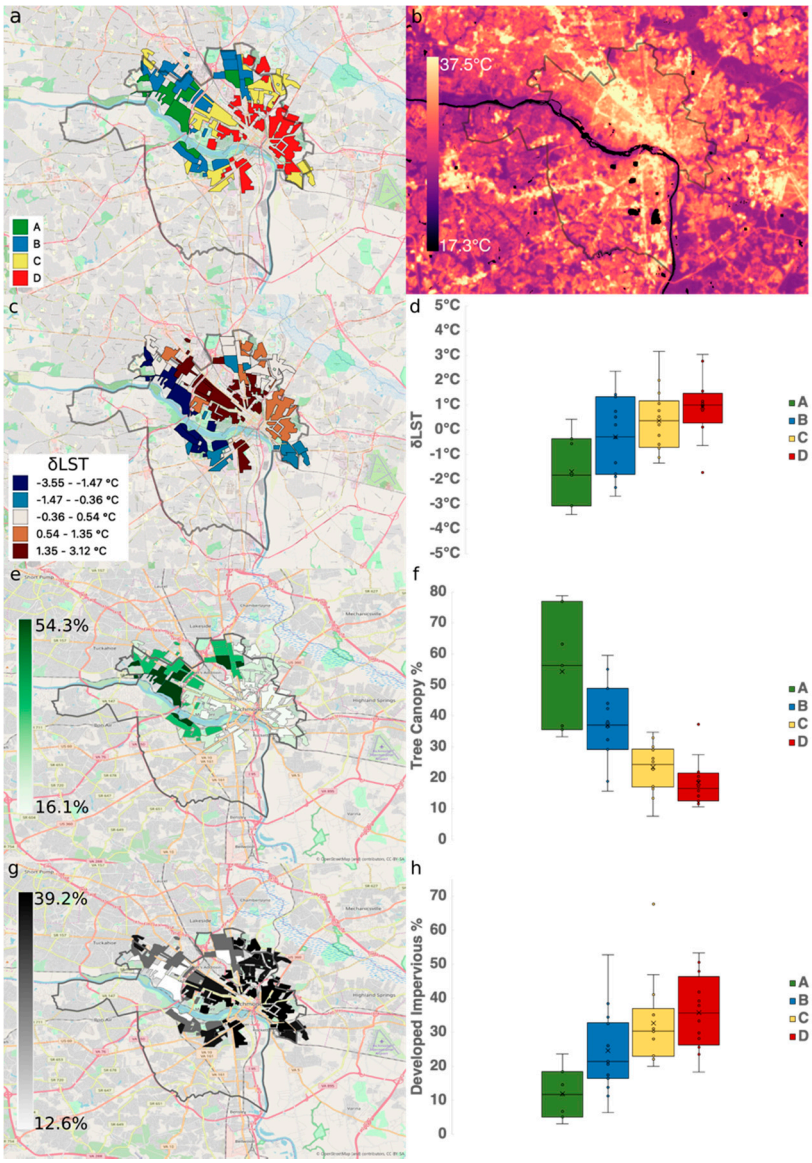

Figure 2. Demonstration of HOLC Security Grade δLST and land cover analysis for Richmond, VA (grey outline). (**a**) HOLC Polygons for Richmond, VA [29] (see Introduction text for explanations of HOLC security grade color designations), (**b**) LST map for Richmond, VA derived from Landsat 8 TIRS Band 10 imagery collected on 2 July 2016, and (**c**) Resulting δLSTs in HOLC polygons calculated as the anomaly of an individual HOLC polygon to the city-wide HOLC polygon average LST (see Equation (1)), (**d**) box–whisker plot of the δLSTs presented in (**c**) binned by HOLC security rating (see Introduction text for explanations of designations), (**e**) percent tree canopy from NLCD 2011 [36] averaged into HOLC polygons, (**f**) box–whisker plot of the δLSTs presented in (**e**) binned by HOLC security rating, (**g**) percent developed impervious surface from NLCD 2011 [36] averaged into HOLC polygons, (**h**) box–whisker plot of the average imperviousness presented in (**g**) binned by HOLC security rating.

3. Results

Our LST maps were generated from Landsat 8 acquisitions that satisfied a < 10 percent scene cloud coverage threshold collected from 3 June 2014 to 25 August 2017 (Supplementary Materials Table S1). These mostly sunny days provide the best conditions for Landsat 8 to reliably capture a strong LST pattern in urban areas [32]. Approximately 40 percent of the Landsat 8 imagery was collected during the 2016 northern hemisphere summer, while ~10 percent of the imagery was collected during the 2014

northern hemisphere summer. Regression tests reveal an insignificant relationship between the day that the imagery was collected and the resulting δLST patterns (Supplementary Materials Table S1).

Our analysis reveals three major trends that help to address our research questions. First, LST differences across the cities follow a non-uniform distribution of differences, suggesting that historical redlining policies are reflected in present-day intra-urban heat differentially (Supplementary Materials Table S1). Notable, intra-city δLST differences between areas given "D" and "A" HOLC security ratings range between +7.1 °C (Portland, OR) to −1.5 °C (Joliet, IL, USA), with ~94% of urban areas included in this study showing warmer present-day LSTs in their "D"-rated areas relative to their "A"-rated areas (Supplementary Materials Table S1). While Portland (OR) and Denver (CO) had the greatest "D" to "A" security rating differences within a city, the warmest δLST temperatures in formerly redlined areas relative to the city-wide average LST were identified in Chattanooga (TN, 3.3 °C) and Baltimore (MD, 3.2 °C). These cities were in contrast to formerly redlined areas that displayed, on average, cooler surface temperatures than their non-redlined counterparts (e.g., Joliet, IL, USA and Lima, OH, USA), a consistent pattern in several cities across the Midwest (Supplementary Materials Table S1). Patterns of relatively pronounced or muted δLST are underscored by attendant patterns of land use type and cover within the same HOLC security rating polygons, whereby the urban areas with the highest D-A difference and largest δLST in D-rated polygons show considerable HOLC rating-specific trends in average tree canopy and developed impervious surface percentages as compared to the Midwestern cities that exhibit cooler-than-average δLST patterns in their D-rated areas (Supplementary Materials Figure S1). The coolest δLST temperatures in areas assigned "A" HOLC security ratings relative to the city-wide average LST were identified in Birmingham (AL, −4.7 °C) and Roanoke (VA, −4.5 °C).

Regional aggregation of the city-specific trends reveals that average δLST differences between HOLC security rating categories exhibit a pattern of incremental warming relative to worsening HOLC security rating (Figure 3b–e). However, the magnitude of the δLST differences varies considerably by region, with the Midwest (n = 41) showing more muted δLST differences than the Southeast (n = 29) and West (n = 12), respectively (Figure 3b–e). Honest Significant Difference tests on urban areas at the regional scale reveal that the greatest δLST differences exist between "A" and "D" HOLC security rating areas across US regions, with "D"-rated areas progressively warmer than each subsequent rating in the present day. These amplified differences in the West and Southeast, as well as the relatively muted response in the Midwest (Figure 3b–e), are attended by similar differences in underlying percent land use cover (Figure 4b–e), and especially apparent in the available tree canopy (Figure 5b–e) for the areas assigned "A" HOLC security ratings.

A third trend that is consistent in a national-scale aggregation of δLSTs in these cities is the finding that "D"-rated areas are now on average 2.6 °C warmer than "A"-rated areas (Figure 3a). Each HOLC security rating category warms systematically relative to the more favorable neighbor security rating category (Figure 3a). Honest Significant Difference tests reveal that areas given "D" HOLC security ratings are significantly warmer than all of the other HOLC security rating categories at the national scale, in progressively larger magnitudes. These LST differences are underscored by similar, but opposing, national-scale patterns in underlying land use and tree canopy within the same redlined cities (Figures 4a and 5a), showing that areas assigned a "hazardous" HOLC security rating in US cities exhibit quantitatively less coverage by tree canopy and more coverage by impervious surfaces in the present decade [35,36].

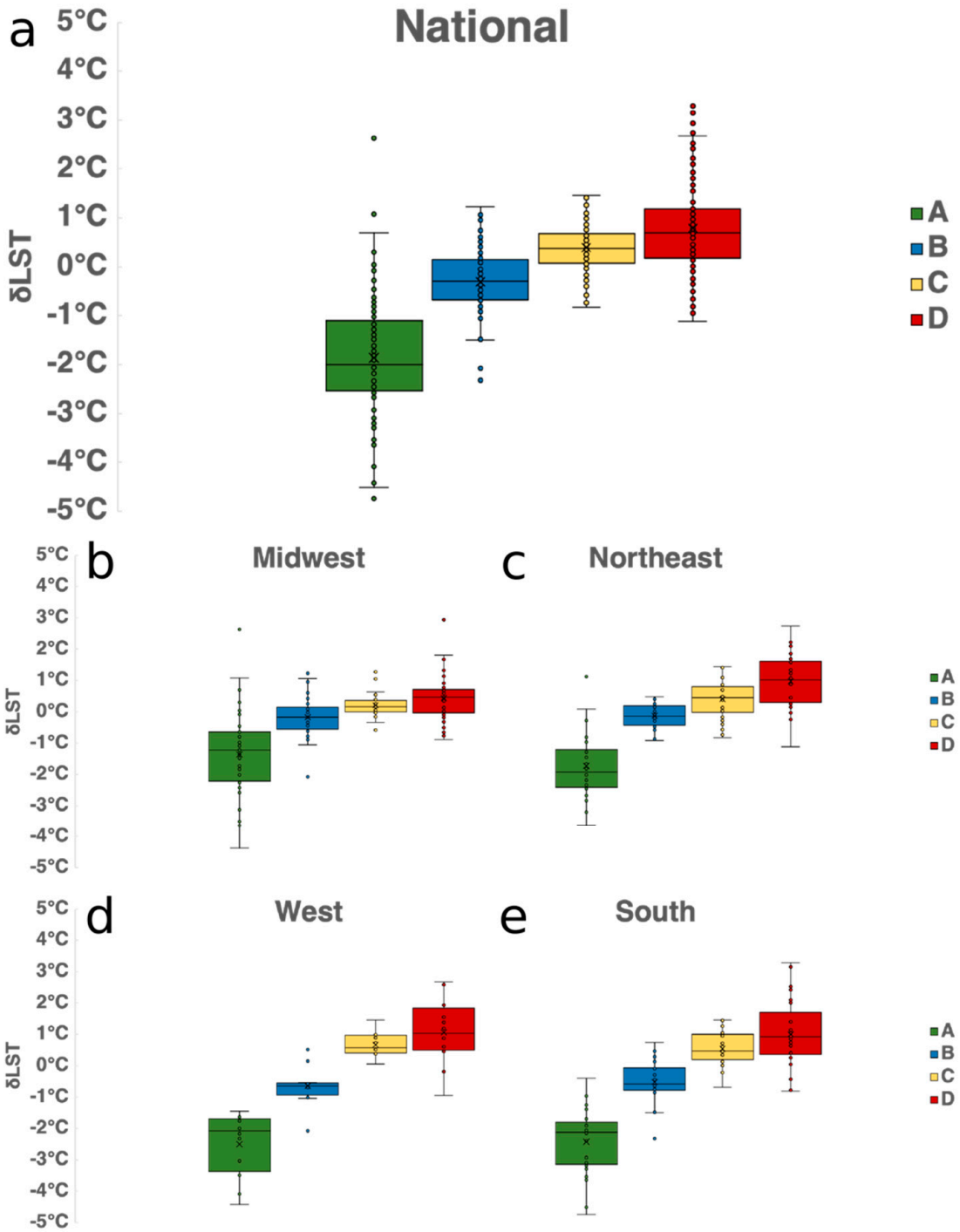

Figure 3. (**a**) National-scale Land Surface Temperature Anomalies by HOLC security rating (Green, "Best," A; Blue, "Still Desirable," B; Yellow, "Definitely Declining," C; Red, "Hazardous," D) (**b**) same as (**a**), but for the Midwest region; (**c**) same as (**b**), but for Northeast region; (**d**) same as (**b**), but for West region; (**e**) same as (**b**), but for South region.

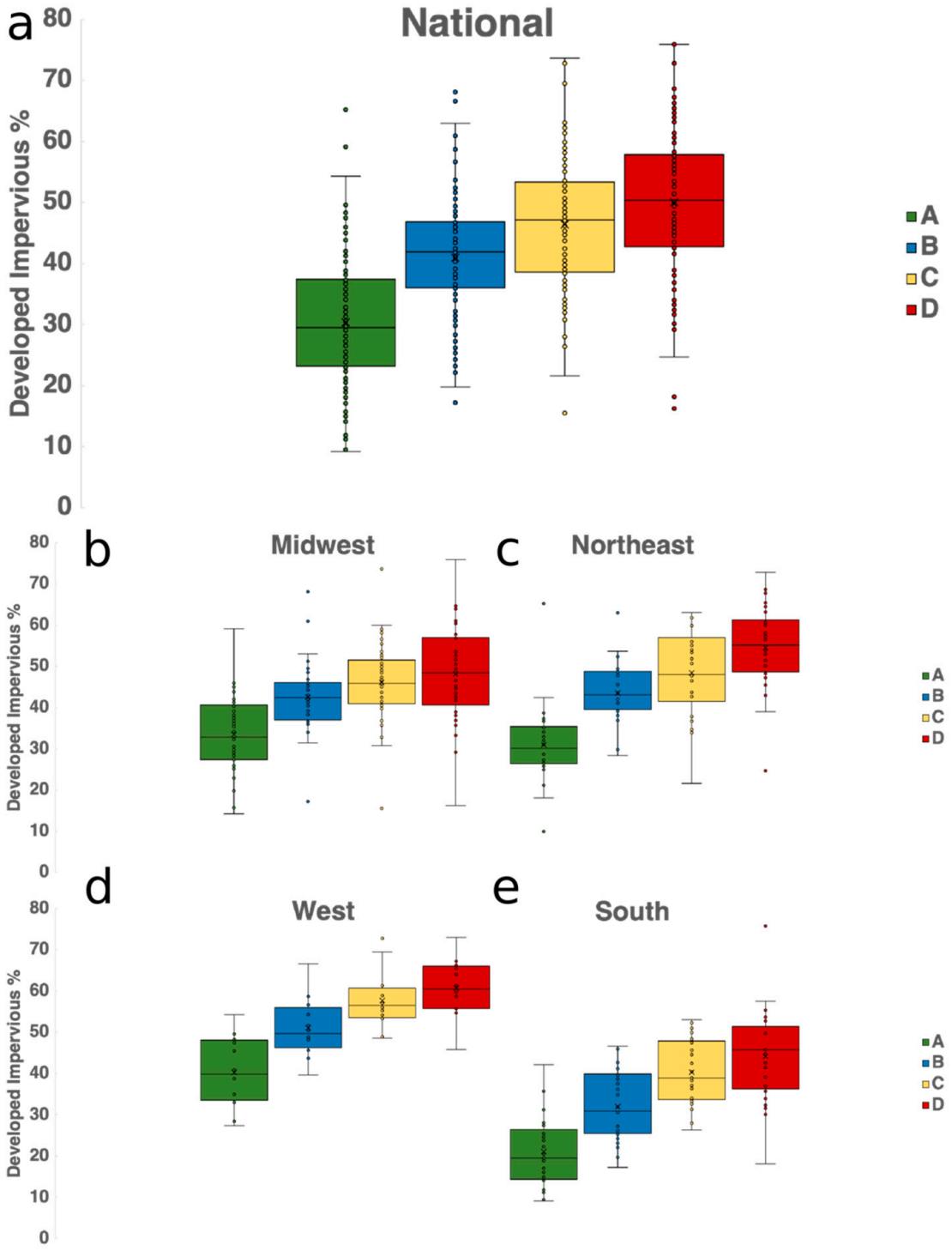

Figure 4. (**a**) National-scale averages of underlying percent developed impervious surface [36] by HOLC security rating (Green, "Best," A; Blue, "Still Desirable," B; Yellow, "Definitely Declining," C; Red, "Hazardous," D), (**b**) same as (**a**), but for the Midwest region; (**c**) same as (**b**), but for Northeast region; (**d**) same as (**b**), but for West region; (**e**) same as (**b**), but for South region.

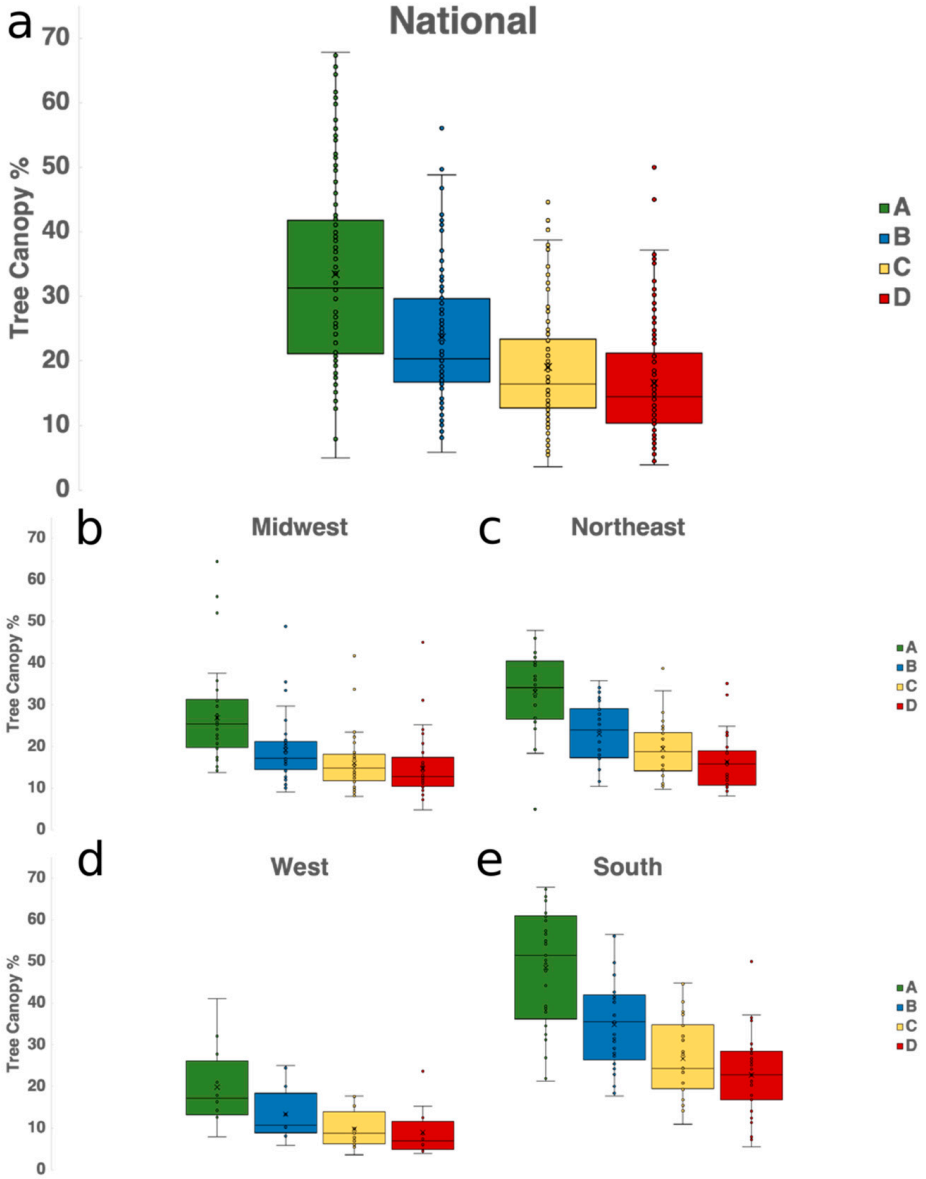

Figure 5. (**a**) National-scale averages of percent tree canopy [35,36] by HOLC security rating (Green, "Best," A; Blue, "Still Desirable," B; Yellow, "Definitely Declining," C; Red, "Hazardous," D), (**b**) same as (**a**), but for the Midwest region; (**c**) same as (**b**), but for Northeast region; (**d**) same as (**b**), but for West region; (**e**) same as (**b**), but for South region.

4. Discussion and Conclusions

We sought to understand the extent to which historic policies of redlining help to explain current patterns of intra-urban heat and the extent to which these patterns were consistent across US cities. Questions about the increasing economic inequality in US society motivated our inquiry and suggest several patterns related to historical federal housing policies and which communities experience the hottest areas of a city in the present day. Most notably, the consistency of greater temperature in formerly redlined areas across the vast majority (94%) of the cities included in this study indicates that current maps of intra-urban heat echo the legacy of past planning policies. While earlier studies document the lack of present-day services for and lower income of communities living in formerly redlined areas, this analysis presents an argument for understanding how global climate change will further exacerbate existing, historically-codified inequities in the US. We highlight three important

dimensions of our findings—built environment, policies, and current inequities—as they relate to implications of these results.

First, our findings corroborate earlier studies that describe consistent patterns between the lack of tree canopy and historically underserved urban areas, at the national and regional scales (Figures 4 and 5). The prevalence of impervious surfaces as opposed to tree canopy points to the fact that green spaces have been consistently more abundant in wealthier and majority White-identifying neighborhoods [26]. At the same time, intra-urban heat is not only affected by tree cover, since the use of different materials within varying urban typologies also amplifies temperatures [19,37]. Two features of the urban landscape—roadways and large building complexes—are well known to transform solar radiation into heat. These landscape features absorb the energy-filled short-wave radiation coming from the sun, and re-emit long-wave radiation during the diurnal heating-cooling process. As a result, large roadways and building complexes gain heat during the day and, as the evening cools ambient temperatures, the retained heat is released back into the neighborhoods, which is captured by overhead satellite sensors. These evening temperatures are precisely the factors that can exacerbate excess mortality and morbidity [38].

An earlier body of evidence from the regional studies and economics literature makes the connection between federal programs that provided incentives for major roadway and building construction projects and the fact that many of these occurred in the lowest income neighborhoods of cities [39–41]. In fact, the 1950s were an important decade for the creation of major roadways across the US, and many redlined neighborhoods were transformed and divided by road and highway infrastructure projects [42]. These changes came at a time when intra-urban heat was not recognized as a major public health hazard, and yet, given the well-known heat-absorbing capacity of asphalt and concrete [43], the selection of these materials may underlie the differences revealed in these results.

Similarly, throughout the mid-1900s large building complexes, including housing complexes, industries, and university campuses, often subsidized by the federal government, were also placed in redlined areas, largely due to the inexpensive land, and current population of largely lower income and communities of color [44]. From the 1940s through the 1970s, large buildings were made of high-density materials, such as cinder block and brick, which retain heat, and maintain high temperatures through the night [45,46]. Many of these buildings still stand, and the LST maps investigated here partially describe the thermal signature of these buildings. Areas that were in non-redlined areas, often built of other materials but also dispersed across a more natural, maintained landscape, which allows for greater circulation of air [47,48] are hence the cooler neighborhoods registered by satellites.

Second, differences in implementing policies and landscapes may help to explain the variation of temperatures across different regions of the US. The cities of Portland (OR), Denver (CO), and Minneapolis (MN), for example, notably reflect the largest differences between the formerly redlined areas and their non-redlined counterparts (Supplementary Materials Table S1). We can speculate that the redlined areas of all three cities are currently located in areas with extensive physical infrastructure, including housing complexes, railway terminals, industrial or manufacturing sites, and/or adjacent to major business centers. The presence of these current day land uses may suggest a relationship between formerly inexpensive land and large-scale development. These results, when combined with more pernicious modern-day policies that support development of high-asphalt and low tree canopy areas such as massive shopping complexes that contain large surface parking lots, are further strengthened. In Portland (OR), for example, decades of development code allowed for multifamily complexes to cover 100% of the lot area with no provisions for greening. Only recently, and due to extensive support from local researchers and community organizations did the city evaluate earlier asphalt-driving policy to require 85% lot coverage and green spaces [49,50]. Such reversals of policy are the forms of planning that can help to reverse decades of amplifying temperatures in areas that have historically been underserved. Denver and Minneapolis are also making strides, though without further understanding about the historic and present-day drivers that generate these asphalt-rich and tree canopy-poor land uses on intra-urban heat, and local communities, progress will be slow.

In addition, the coupling of landscape and historic designs of urban development in these cities may also play a role in helping to explain differences across the country. Portland, like Minneapolis, are in landscapes where tree canopy is relatively easy to sustain. Unlike arid and drought-prone areas, where planting trees can require extensive maintenance, the warm, sunny summers and wet/snowy winters of Portland, Minneapolis and other cities of the Northwest and Midwest, provide ideal conditions for expanding an urban forest, which can, in turn, reduce surface temperatures of a neighborhood. Tree planting efforts often took place as part of urban development projects in the early and mid-1900s, and were used as a way to mark special designations [42]. Similarly, metropolitan areas that conform to the concentric zone model (for example, places like Chicago, Los Angeles, and Philadelphia) tend to be larger and more densely populated metros, often with a higher degree of both affluence and inequality, a larger African American population, and a greater share of population in the suburbs. In the remaining metropolitan areas, there is greater integration between the affluent and the poor [44]. In these places, such as Seattle (WA), Charleston (WV), and Birmingham (AL), the rich are concentrated in the urban core, where redlining and tree planting efforts coincide.

Finally, indicators of and/or higher intra-urban LSTs have been shown to correlate with higher summertime energy use [51,52], and excess mortality and morbidity [20,53,54]. The fact that residents living in formerly redlined areas may face higher financial burdens due to higher energy and more frequent health bills further exacerbates the long-term and historical inequities of present and future climate change. As the results from earlier studies have documented income inequality between formerly redlined areas another other parts of US cities, we recognize that hotter areas will amplify these current inequities. Such historic income inequality leads to income segregation because higher incomes, which are further supported by past and current housing policy, allow certain households to sort themselves according to their preferences—and control local political processes that continue exclusion [55]. Other explanatory factors of these patterns, though too many for the current study and setting the stage for future studies, include disinvestment in urban areas, suburban investment and land use patterns, and the practices generally of government and the underwriting industry [39,56].

To our knowledge, this is the first study to link a historical federal housing policy to the creation (or at least the exacerbation) of a climate stressor and potential variability in resident exposure to it. While redlining most likely did not create the microenvironments that mediate LSTs relative to the rest of the urban environment, our findings suggest a strong and significant likelihood of the cauterization of current day exposure to the hottest parts of a city. While patterns of who experiences the most exposure to intra-urban heat may change as a result of (green) gentrification, which many formerly redlined neighborhoods are undergoing (e.g., wealthier communities can afford to green and change the physical landscape, and, over time, cool the hottest areas of a city), we observe consistent patterns that can be inferred as in part due to the creation of HOLC maps [23]. Future studies will need to describe the mechanisms by with planning practices—past and present—are likely to amplify the effects of climate change on historically underserved communities and communities of color.

While a growing body of evidence describes the intra-urban variation of temperatures due to characteristics of the built environment, few have asked why we observe a pattern of historically-marginalized communities living in the hottest areas. Here we have presented results from an analysis of 108 US cities that aimed to examine the role of historic "redlining" policies in mediating exposure to intra-urban heat. We found that in nearly all cases, those neighborhoods located in formerly redlined areas—that remain predominantly lower income and communities of color—are at present hotter than their non-redlined counterparts. Although the extent of differences in temperatures varies by region, the preponderance of evidence establishes that those experiencing the greatest exposure to present and potentially future extreme heat are living in neighborhoods with the least social and ecosystem services historically.

As more and more communities race to develop plans to react to and adapt to worsening extreme heat and its attendant effects on human health [57], a research agenda focused on developing place-specific, heat-mitigating urban designs and interventions [58–61] will be critical toward not

only alleviating heat disparity but ensuring that the urban forms and policies that gave rise to these inequities in our past (like redlining) are recognized and altogether avoided. Furthermore, crafting climate equity-centered policies that recognize decades of disproportionate exposure to environmental stressors can help any new discoveries in urban design get implemented with focus and rapidity.

Supplementary Materials: The following are available online at http://www.mdpi.com/2225-1154/8/1/12/s1, Figure S1: Comparison of urban areas of relatively large or small differences in LSTs between HOLC grades, Table S1: Urban area-specific results from our LST analysis.

Author Contributions: J.S.H. conceived the project and coordinated the analysis, advised interpretation, and contributed to the manuscript, created figures, and coordinated the responses to reviewers. V.S. provided major contributions to the manuscript including context, interpretation, editorialization, and literature review and references. N.P. performed HOLC map and satellite imagery download and spatial analyses. All authors have read and agreed to the published version of the manuscript.

Funding: This research involved no external funding.

Acknowledgments: J.S.H. thanks the NOAA Office of Education Environmental Literacy Program, the Virginia Academy of Science, Groundwork RVA, Virginia Commonwealth University SustainLab, University of Richmond Spatial Analysis and Digital Scholarship Labs, and the City of Richmond Sustainability Office. J.S.H. and V.S. acknowledge support from the NOAA Climate Program Office, and U.S. Forest Service's National Urban and Community Forestry Challenge Grants Program (No. 17-DG-11132544-014). N.P. acknowledges the work study program at the Virginia Commonwealth University. The authors thank four anonymous reviewers for their thoughtful and thorough consideration.

Conflicts of Interest: The authors declare no conflict of interest.

References

1. Wong, K.V.; Paddon, A.; Jimenez, A. Review of World Urban Heat Islands: Many Linked to Increased Mortality. *Energy Resour. Technol.* **2013**, *135*, 022101. [CrossRef]
2. Poumadère, M.; Mays, C.; Le Mer, S.; Blong, R. The 2003 Heat Wave in France: Dangerous Climate Change Here and Now. *Risk Anal.* **2005**, *25*, 1483–1494. [CrossRef]
3. Borden, K.A.; Cutter, S.L. Spatial patterns of natural hazards mortality in the United States. *Int. J. Health Geogr.* **2008**, *7*, 64. [CrossRef]
4. Hess, J.J.; Eidson, M.; Tlumak, J.E.; Raab, K.K.; George, L. An evidence-based public health approach to climate change adaptation. *Environ. Health Perspect.* **2014**, *122*, 1177–1186. [CrossRef]
5. Uejio, C.K.; Wilhelmi, O.V.; Golden, J.S.; Mills, D.M.; Gulino, S.P.; Samenow, J.P. Intra-urban societal vulnerability to extreme heat: The role of heat exposure and the built environment, socioeconomics, and neighborhood stability. *Health Place* **2011**, *17*, 498–507. [CrossRef]
6. Habeeb, D.; Vargo, J.; Stone, B. Rising heat wave trends in large US cities. *Nat. Hazards* **2015**, *76*, 1651–1665. [CrossRef]
7. Wang, Y.; Wang, A.; Zhai, J.; Tao, H.; Jiang, T.; Su, B.; Yang, J.; Wang, G.; Liu, Q.; Gao, C.; et al. Tens of thousands additional deaths annually in cities of China between 1.5 °C and 2.0 °C warming. *Nat. Commun.* **2019**, *10*, 3376. [CrossRef] [PubMed]
8. Meehl, G.A.; Tebaldi, C. More Intense, More Frequent, and Longer Lasting Heat Waves in the 21st Century. *Science* **2004**, *305*, 994. [CrossRef] [PubMed]
9. Santamouris, M. Analyzing the heat island magnitude and characteristics in one hundred Asian and Australian cities and regions. *Sci. Total Environ.* **2015**, *512–513*, 582–598. [CrossRef]
10. Lo, Y.T.E.; Mitchell, D.M.; Gasparrini, A.; Vicedo-Cabrera, A.M.; Ebi, K.L.; Frumhoff, P.C.; Millar, R.J.; Roberts, W.; Sera, F.; Sparrow, S.; et al. Increasing mitigation ambition to meet the Paris Agreement's temperature goal avoids substantial heat-related mortality in U.S. cities. *Sci. Adv.* **2019**, *5*, eaau4373. [CrossRef] [PubMed]
11. Voelkel, J.; Shandas, V.; Haggerty, B. Developing High-Resolution Descriptions of Urban Heat Islands: A Public Health Imperative. *Prev. Chronic Dis.* **2016**, *13*, E129. [CrossRef]
12. Ziter, C.D.; Pedersen, E.J.; Kucharik, C.J.; Turner, M.G. Scale-dependent interactions between tree canopy cover and impervious surfaces reduce daytime urban heat during summer. *Proc. Natl. Acad. Sci. USA* **2019**, *116*, 7575. [CrossRef]

13. Shandas, V.; Voelkel, J.; Williams, J.; Hoffman, J. Integrating Satellite and Ground Measurements for Predicting Locations of Extreme Urban Heat. *Climate* **2019**, *7*, 5. [CrossRef]
14. Li, X.; Zhou, Y.; Asrar, G.R.; Imhoff, M.; Li, X. The surface urban heat island response to urban expansion: A panel analysis for the conterminous United States. *Sci. Total Environ.* **2017**, *605–606*, 426–435. [CrossRef]
15. Li, Y.-Y.; Zhang, H.; Kainz, W. Monitoring patterns of urban heat islands of the fast-growing Shanghai metropolis, China: Using time-series of Landsat TM/ETM+ data. *Int. J. Appl. Earth Obs. Geoinf.* **2012**, *19*, 127–138. [CrossRef]
16. Davis, A.Y.; Jung, J.; Pijanowski, B.C.; Minor, E.S. Combined vegetation volume and "greenness" affect urban air temperature. *Appl. Geogr.* **2016**, *71*, 106–114. [CrossRef]
17. Jun, M.-J.; Kim, J.-I.; Kim, H.-J.; Yeo, C.-H.; Hyun, J.-Y. Effects of Two Urban Development Strategies on Changes in the Land Surface Temperature: Infill versus Suburban New Town Development. *J. Urban Plann. Dev.* **2017**, *143*, 04017010. [CrossRef]
18. Aram, F.; Higueras García, E.; Solgi, E.; Mansournia, S. Urban green space cooling effect in cities. *Heliyon* **2019**, *5*, e01339. [CrossRef]
19. Hamstead, Z.A.; Kremer, P.; Larondelle, N.; McPhearson, T.; Haase, D. Classification of the heterogeneous structure of urban landscapes (STURLA) as an indicator of landscape function applied to surface temperature in New York City. *Ecol. Indic.* **2016**, *70*, 574–585. [CrossRef]
20. Madrigano, J.; Ito, K.; Johnson, S.; Kinney, P.L.; Matte, T. A Case-Only Study of Vulnerability to Heat Wave–Related Mortality in New York City (2000–2011). *Environ. Health Perspect.* **2015**, *123*, 672–678. [CrossRef]
21. Voelkel, J.; Hellman, D.; Sakuma, R.; Shandas, V. Assessing Vulnerability to Urban Heat: A Study of Disproportionate Heat Exposure and Access to Refuge by Socio-Demographic Status in Portland, Oregon. *IJERPH* **2018**, *15*, 640. [CrossRef]
22. Whitman, S.; Good, G.; Donoghue, E.R.; Benbow, N.; Shou, W.; Mou, S. Mortality in Chicago attributed to the July 1995 heat wave. *Am. J. Public Health* **1997**, *87*, 1515–1518. [CrossRef]
23. Aaronson, D.; Hartley, D.; Mazumder, B. The Effects of the 1930s HOLC "Redlining" Maps. In *Federal Reserve Bank of Chicago Working Paper No. 2017-12*; Federal Reserve Bank of Chicago: Chicago, IL, USA, 2017; pp. 1–102.
24. Mitchell, B.; Franco, J. *HOLC "Redlining" Maps: The Persistent Structure of Segregation and Economic Inequality*; National Community Reinvestment Coalition: Washington, DC, USA, 2018; pp. 1–29.
25. Lipsitz, G. *How Racism Takes Place*; Temple University Press: Philadelphia, PA, USA, 2011.
26. Nowak, D.J.; Greenfield, E.J. Declining urban and community tree cover in the United States. *Urban For. Urban Green.* **2018**, *32*, 32–55. [CrossRef]
27. Schwarz, K.; Fragkias, M.; Boone, C.G.; Zhou, W.; McHale, M.; Grove, J.M.; O'Neil-Dunne, J.; McFadden, J.P.; Buckley, G.L.; Childers, D.; et al. Trees Grow on Money: Urban Tree Canopy Cover and Environmental Justice. *PLoS ONE* **2015**, *10*, e0122051. [CrossRef]
28. Nardone, A.; Thakur, N.; Balmes, J.R. Historic Redlining and Asthma Exacerbations across Eight Cities of California: A Foray into How Historic Maps Are Associated with Asthma Risk. *Am. J. Resp. Crit. Care Med* **2019**, *199*, A7054.
29. Nelson, R.K.; Winling, L.; Marciano, R.; Connolly, N. Mapping Inequality: Redlining in New Deal America. Available online: https://dsl.richmond.edu/panorama/redlining/ (accessed on 9 October 2017).
30. Avdan, U.; Jovanovska, G. Algorithm for Automated Mapping of Land Surface Temperature Using LANDSAT 8 Satellite Data. *J. Sens.* **2016**, *2016*, 1–8. [CrossRef]
31. Cook, M.; Schott, J.; Mandel, J.; Raqueno, N. Development of an Operational Calibration Methodology for the Landsat Thermal Data Archive and Initial Testing of the Atmospheric Compensation Component of a Land Surface Temperature (LST) Product from the Archive. *Remote Sens.* **2014**, *6*, 11244–11266. [CrossRef]
32. Sheng, L.; Tang, X.; You, H.; Gu, Q.; Hu, H. Comparison of the urban heat island intensity quantified by using air temperature and Landsat land surface temperature in Hangzhou, China. *Ecol. Indic.* **2017**, *72*, 738–746. [CrossRef]
33. White-Newsome, J.L.; Brines, S.J.; Brown, D.G.; Dvonch, J.T.; Gronlund, C.J.; Zhang, K.; Oswald, E.M.; O'Neill, M.S. Validating Satellite-Derived Land Surface Temperature with *in situ* Measurements: A Public Health Perspective. *Environ. Health Perspect.* **2013**, *121*, 925–931. [CrossRef]

34. Yang, L.; Huang, C.; Homer, C.G.; Wylie, B.K.; Coan, M.J. An approach for mapping large-area impervious surfaces: Synergistic use of Landsat-7 ETM+ and high spatial resolution imagery. *Can. J. Remote Sens.* **2014**, *29*, 230–240. [CrossRef]
35. Coulston, J.W.; Moisen, G.G.; Wilson, B.T.; Finco, M.V.; Cohen, W.B.; Brewer, C.K. Modeling percent tree canopy cover: A pilot study. *Photogramm. Eng. Remote Sens.* **2012**, *78*, 715–727. [CrossRef]
36. Homer, C.G.; Dewitz, J.; Yang, L.; Jin, S.; Danielson, P.; Xian, G.Z.; Coulston, J.; Herold, N.; Wickham, J.; Megown, K. Completion of the 2011 National Land Cover Database for the conterminous United States—Representing a decade of land cover change information. *Photogramm. Eng. Remote Sens.* **2015**, *81*, 345–354.
37. Stewart, I.D.; Oke, T.R. Local Climate Zones for Urban Temperature Studies. *Bull. Am. Meteor. Soc.* **2012**, *93*, 1879–1900. [CrossRef]
38. Murage, P.; Hajat, S.; Kovats, R.S. Effect of night-time temperatures on cause and age-specific mortality in London. *Environ. Epidemiol.* **2017**, *1*. [CrossRef]
39. Hirsch, A. *Making the Second Ghetto: Race and Housing in Chicago, 1940–1960*; Cambridge University Press: New York, NY, USA, 1983.
40. Teaford, J.C. *The Rough Road to Renaissance: Urban Revitalization in America, 1940–1985*; Johns Hopkins University Press: Baltimore, MD, USA, 1990.
41. Sugrue, T.J. *The Origins of the Urban Crisis: Race and Inequality in Postwar Detroit*; Princeton University Press: Princeton, NJ, USA, 1996.
42. DiMento, J.F.C. Stent (or Dagger?) in the Heart of Town: Urban Freeways in Syracuse, 1944–1967. *J. Plan. Hist.* **2009**, *8*, 133–161. [CrossRef]
43. Swaid, H. Numerical investigation into the influence of geometry and construction materials on urban street climate. *Phys. Geogr.* **2013**, *14*, 342–358. [CrossRef]
44. Zuk, M.; Bierbaum, A.H.; Chapple, K.; Gorska, K.; Loukaitou-Sideris, A. Gentrification, Displacement, and the Role of Public Investment. *J. Plan. Lit.* **2017**, *33*, 31–44. [CrossRef]
45. Kim, H.H. Urban heat island. *Int. J. Remote Sens.* **1992**, *13*, 2319–2336. [CrossRef]
46. Hall, J.P. *The Early Developmental History of Concrete Block in America*; Ball State University Library: Muncie, IN, USA, 2009.
47. Howard, B.; Parshall, L.; Thompson, J.; Hammer, S.; Dickinson, J.; Modi, V. Spatial distribution of urban building energy consumption by end use. *Energy Build.* **2012**, *45*, 141–151. [CrossRef]
48. Barrington-Leigh, C.; Millard-Ball, A. A century of sprawl in the United States. *Proc. Natl. Acad. Sci. USA* **2015**, *112*, 8244–8249. [CrossRef]
49. Anderson, M. In Mid-Density Zones, Portland Has a Choice: Garages or Low Prices? Available online: https://www.sightline.org/2019/10/02/in-mid-density-zones-portland-has-a-choice-garages-or-low-prices/ (accessed on 14 October 2019).
50. Better Housing by Design. Available online: https://www.portlandoregon.gov/bps/71903 (accessed on 14 October 2019).
51. Lowe, S.A. An energy and mortality impact assessment of the urban heat island in the US. *Environ. Impact Assess. Rev.* **2016**, *56*, 139–144. [CrossRef]
52. Li, X.; Zhou, Y.; Yu, S.; Jia, G.; Li, H.; Li, W. Urban heat island impacts on building energy consumption: A review of approaches and findings. *Energy* **2019**, *174*, 407–419. [CrossRef]
53. Chuang, W.-C.; Gober, P. Predicting Hospitalization for Heat-Related Illness at the Census-Tract Level: Accuracy of a Generic Heat Vulnerability Index in Phoenix, Arizona (USA). *Environ. Health Perspect.* **2015**, *123*, 606–612. [CrossRef]
54. Eisenman, D.P.; Wilhalme, H.; Tseng, C.-H.; Chester, M.; English, P.; Pincetl, S.; Fraser, A.; Vangala, S.; Dhaliwal, S.K. Heat Death Associations with the built environment, social vulnerability and their interactions with rising temperature. *Health Place* **2016**, *41*, 89–99. [CrossRef]
55. Reardon, S.F.; Bischoff, K. Income Inequality and Income Segregation. *Am. J. Sociol.* **2011**, *116*, 1092–1153. [CrossRef]
56. Levy, D.K.; McDade, Z.; Dumlao, K. *Effects from Living in Mixed-Income Communities for Low-Income Families*; Urban Institute: Washington, DC, USA, 2011; p. 34.
57. Martinez, G.S.; Linares, C.; Ayuso, A.; Kendrovski, V.; Boeckmann, M.; Diaz, J. Heat-health action plans in Europe: Challenges ahead and how to tackle them. *Environ. Res.* **2019**, *176*, 108548. [CrossRef]

58. Makido, Y.; Hellman, D.; Shandas, V. Nature-Based Designs to Mitigate Urban Heat: The Efficacy of Green Infrastructure Treatments in Portland, Oregon. *Atmosphere* **2019**, *10*, 282. [CrossRef]
59. Hatvani-Kovacs, G.; Belusko, M.; Pockett, J.; Boland, J. Heat stress-resistant building design in the Australian context. *Energy Build.* **2018**, *158*, 290–299. [CrossRef]
60. Alam, M.; Sanjayan, J.; Zou, P.X.W. Chapter Eleven—Balancing Energy Efficiency and Heat Wave Resilience in Building Design. In *Climate Adaptation Engineering*; Bastidas-Arteaga, E., Stewar, M.G., Eds.; Butterworth-Heinemann: Oxford, UK, 2019; pp. 329–349.
61. He, B.-J. Towards the next generation of green building for urban heat island mitigation: Zero UHI impact building. *Sustain. Cities Soc.* **2019**, *50*, 101647. [CrossRef]